Proceedings of the Combustion Institute 42 (2026) 106078

Contents lists available at ScienceDirect

Proceedings of the Combustion Institute

journal homepage: www.elsevier.com/locate/proci

Ultra-lean diffusion-controlled 2D premixed hydrogen/air flames

Cheng Chi [a,*], Zheng Chen [b], Dominique Thévenin [a]

[a] Lab. of Fluid Dynamics and Technical Flows, Otto von Guericke University Magdeburg, D-39106, Germany
[b] SKLTCS, HEDPS, School of Mechanics and Engineering Science, Peking University, Beijing, 100871, China

ARTICLE INFO

Keywords:
Hydrogen/air flames
Ultra-lean
Gravity effect
Differential diffusion
Stable premixed flames

ABSTRACT

To facilitate zero-carbon energy with lean hydrogen combustion, 2D ultra-lean premixed hydrogen/air flames (reaching the flammability limit) are systematically studied using Direct numerical simulations (DNS) with detailed models for molecular transport and chemistry. Equivalence ratios ϕ ranging from 0.1 to 0.3 are considered. Gravity effect is also considered. By analyzing the DNS results, novel findings are obtained: (i) Without gravity, diffusion-controlled stable flames are observed at $0.1 \leq \phi \leq 0.2$. As ϕ decreases, the stable cell width decreases and the flame curvature increases, intensifying the differential diffusion focusing effect, thus keeping a certain reactivity for flame stabilization. At smaller ϕ, the flame propagation is dominated by flame tangential differential diffusion. (ii) With gravity in the opposite direction as the flame propagation, the flames at $\phi = 0.1$ and 0.15 become dominated by flame normal differential diffusion, with significantly increased stable cell width. The flame at $\phi = 0.2$ exhibits splitting cell dynamics. (iii) With gravity in the same direction as the flame propagation, the flames at $\phi = 0.2$, 0.25 and 0.3 become unstable. The two-headed cell cannot be stabilized in these 2D flames. These findings are important for a comprehensive understanding of ultra-lean premixed hydrogen/air flames, and are relevant to hydrogen safety and premixed combustion modeling.

Novelty and significance statement: Ultra-lean premixed hydrogen flames have been previously mostly studied in open Hele-Shaw cells and quasi-2D configurations with wall heat loss (Veiga-López et al., 2020; Yang et al., 2025). A previous 2D study (Grcar, 2009) only considered one single equivalence ratio and did not analyze the stabilization mechanism. The present work bridges this knowledge gap by the first-ever systematic 2D study involving various equivalence ratios w/o gravity. Different from most of the previous studies, the configuration in this study does not involve any wall heat loss or radiative heat loss. Novel insights on such flames are obtained: (i) a stability regime for the 2D ultra-lean flames is concluded; (ii) the stabilization and flame cell shape controlling mechanisms are identified; (iii) the effect of gravity is revealed.

Ultra-lean premixed hydrogen flames are very important for hydrogen safety (Yang et al., 2025) and provide a promising theoretical foundation for premixed combustion modeling (Grcar, 2009). The present study significantly extends our knowledge about ultra-lean 2D premixed hydrogen flames and also help to explain the different flame modes in open Hele-Shaw cells or narrow gaps. The results are important to improve hydrogen safety and to support premixed combustion model development under lean conditions.

1. Introduction

To achieve a decarbonized energy transition, lean premixed hydrogen flames have been intensively studied in recent years [1]. One most distinct feature of the lean hydrogen flames is the thermodiffusive instability, induced by the preferential diffusion of H_2 and H. The thermodiffusive instability has thus been investigated extensively (e.g., [2,3]). However, these studies are limited to an equivalence ratio ϕ above 0.3. It was found that the flame becomes stable again when it is even leaner, revealing a stable flame cell at $\phi = 0.2$ in [4] and a flame ball at $\phi < 0.2$ in [5–7].

Both flame cell and flame ball would burn until reaching the lean flammability limit and have significantly low flame temperature, contributing to reduced pollutant emissions. Therefore, these specific flames have gained increasing attention in the combustion community [8–10]. The flame cell was found to be stabilized by convective heat loss [4], while the flame ball was stabilized by radiative heat loss [5,6]. The competition between heat loss and reaction heat generation determines the stability limits. Similar phenomena have been observed for ultra-lean hydrogen flames in narrow gaps or Hele-Shaw cells. There, the competition between wall heat loss and reaction

* Corresponding author.
E-mail address: cheng.chi@ovgu.de (C. Chi).

https://doi.org/10.1016/j.proci.2026.106078
Received 1 March 2026; Accepted 5 June 2026
Available online 25 June 2026

heat generation determines the stable flame topology [11]. In narrow gaps, several stable flame propagation modes were identified and categorized in an experimental study [11], e.g., one-headed steady cells, two-headed steady cells and splitting cells. Similar experimental studies on ultra-lean hydrogen flames in a Hele-Shaw cell also showed that the flame can propagate in one-headed or two-headed finger structures [12,13]. The imbalance between wall heat loss and reaction heat generation explains the splitting mechanism for the splitting cell mode [11]. Quasi-2D simulations [14–17] with a simple molecular diffusion model and single-step chemistry have also been conducted. Both stable two-headed and one-headed cells were identified. More recently, 3D simulations with detailed chemistry and transport models have been done for ultra-lean hydrogen flames in a Hele-Shaw cell [18]. Different cellular flame regimes were identified and interpreted. A theoretical study [19] also proved that the flame cell is a stable solution under heat loss. For all these quasi-2D and 3D flames, the local equivalence ratio ϕ (determining the local reaction heat generation) and the heat loss (by convection, radiation, or wall conduction) control the ultra-lean flame shape and propagation. Additionally, gravity was also found to significantly affect the flame propagation modes [11].

Most of these previous studies focused on flame ball (stabilized by the radiative heat loss) or flame cell (stabilized by the wall heat loss). However, a more general case, the flame cell stabilized by the convective heat loss, was rarely studied. Grcar [4] identified a stable flame cell for a lean H_2/air flame at $\phi = 0.2$ by 2D simulations. This case mimics a 3D flame with adiabatic walls in cross-flow direction for narrow gaps or Hele-Shaw cells. The heat loss is due to convection, instead of wall conduction [4]. Simplifying the 3D problem into a 2D problem is a common practice for such studies [14–17]. Therefore, this 2D configuration is of practical relevance. In this study, the flame cell was found to be stable to higher dimensional perturbations than flame balls or flat flames. Real premixed flames have a natural tendency to exhibit such flame shapes, showing the high significance of this configuration as a theoretical basis from which to develop models of premixed combustion, particularly under ultra-lean conditions [4]. However, the effects of gravity and of further variations in equivalence ratio ϕ have not been examined yet for this flame configuration. Therefore, the present study aims to fill this knowledge gap and to identify and interpret different stable flame propagation modes associated to different ϕ via Direct Numerical Simulations (DNS) of 2D ultra-lean hydrogen flames (without wall heat loss nor radiative heat loss). The effect of gravity is also studied. The premixed H_2/air flames are studied beyond the flammability limit and the resulting stabilization mechanism is revealed.

2. Numerical setup

All the DNS are performed using the in-house combustion solver DINO [20], with detailed molecular transport model (mixture-averaged model considering Soret effect) and chemical mechanism [21]. Radiative heat loss is not considered on purpose, even if it is known to be relevant for other configurations [5,6], in order to concentrate the present study on the convective heat loss. Ultra-lean hydrogen/air flames are simulated at equivalence ratios of $\phi = 0.1, 0.15, 0.2, 0.25$ and 0.3 (corresponding to 4%, 6%, 7.8%, 9.5% and 11.2% H_2 volume ratios, respectively) with an unburned temperature of 300 K and atmospheric pressure. To reach the lean flammability limit, leaner mixtures with $\phi < 0.1$ have also been checked, but they failed to burn. Same as in [4], the simulation begins from a planar premixed flame zone and burnt gas of a richer mixture at $\phi = 0.3$ (Note that planar premixed H_2/air flames with $\phi \leq 0.25$ cannot be established [22]). The flame zone is mapped from the corresponding 1D flame solution. The flame zone quickly adapts to the leaner mixture (on the fresh gas side), and the initially richer exhaust gas is completely flushed out during the simulation. Gravity effect is checked with $g = 9.8$ m/s^2 imposed along (called negative g) or against (called positive g) the flame propagation direction. A sketch

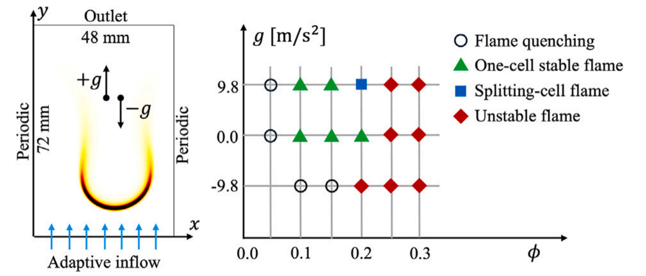

Fig. 1. (Left) Sketch of the numerical configuration and (Right) all the cases considered in this study.

of the numerical configuration and all the cases in this study are shown in Fig. 1. A computational domain with size 48 mm × 72 mm is used, which was found to be large enough to accommodate one stable flame cell at $\phi = 0.2$ [4]. The size of this domain was also confirmed to be large enough for the flames at all other ϕ, as discussed in the later sections. The domain is uniformly discretized by 1536 × 2304 grids, with a resolution of 31.25 μm. This resolution ensures at least 20 grid points within the laminar flame thickness at $\phi = 0.4$, while leaner flames have an even larger flame thickness. The flame is propagating in negative y direction from top to bottom. An adaptive inflow is imposed at the bottom boundary to ensure that the flame is always kept within the domain. Periodic boundary conditions are used in x direction. All the simulations are continued for a sufficiently long physical time, to make sure that the flames are indeed stable, as discussed further in the next section.

Fig. 1 summarizes all the cases in this study. Based on the flame shape and flame propagation dynamics, these cases are categorized into (a) flame quenching; (b) one-cell stable flame; (c) splitting-cell flame; and (d) unstable flame. In general, a stability regime for the ultra-lean H_2 flames can be identified. Similar to the ultra-lean flames in narrow gaps or Hele-Shaw cell, one-cell stable flame and splitting-cell flame can be observed in these 2D cases. More detailed analysis is discussed in the next section.

3. Results and discussion

The simulation results are analyzed in this section. Firstly, the flames without gravity effect are examined. Then, the effect of gravity is analyzed. The flame shape is paid special attention during the analysis.

3.1. Flame propagation with zero gravity

Fig. 2 shows the temporal evolution of flame propagation for the ultra-lean hydrogen flames with zero gravity. For an easier comparison, time $t = 0$ denotes the time when the flames have been found to be stable. For unstable flames, $t = 0$ is chosen when the flames are quasi-steady. As is seen, stable flame cap structures are observed when $\phi = 0.1, 0.15$ and 0.2. These flame structures retain their shapes for several seconds in physical time (corresponding to more than 10 flame time scales $t_f = \delta_C/S_C$ of the corresponding flames), demonstrating their stable feature. Here, δ_C and S_C are the maximum thermal flame thickness and propagation speed of the cell flame respectively. Note that the flame cells are not necessarily in the middle of the domain because of the initialization using the unstable flame at $\phi = 0.3$. When ϕ increases to 0.25 and 0.3, typical thermodiffusive unstable cellular flames are observed, with enhanced peak heat release rate (HRR – note the different color scales in Fig. 2). The transition from stable to unstable flame happens between $\phi = 0.2$ and $\phi = 0.25$.

For those ultra-lean stable flames, the flame propagation is largely controlled by preferential diffusion of H_2. Therefore, we call those

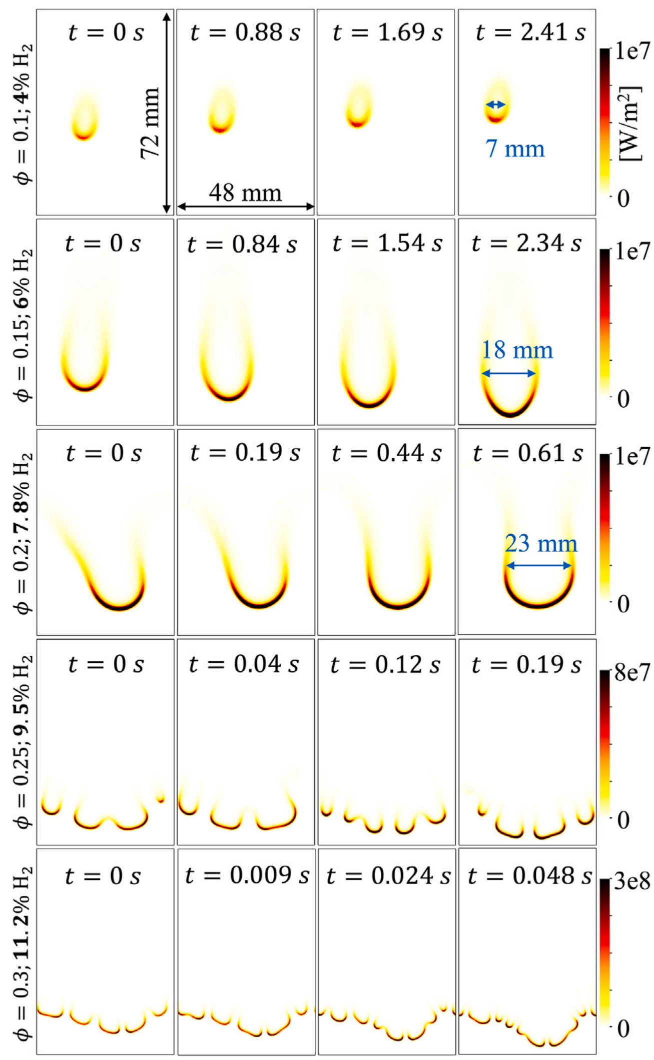

Fig. 2. Flame propagation with time for lean hydrogen flames with equivalence ratio $\phi = 0.1, 0.15, 0.2, 0.25$ and 0.3 from top to bottom. No gravity is considered.

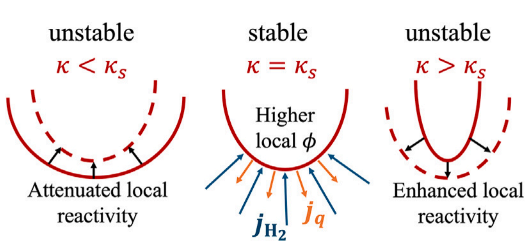

Fig. 3. Sketch showing the stabilization mechanism of the diffusion-controlled ultra-lean hydrogen/air flames as function of flame curvature κ. The solid red line represents the current flame position, while the dashed red line represents the stable flame position. The black arrows indicate the development trend of the flame shape.

"diffusion-controlled" flames. As ϕ increases, the successful flame propagation becomes less dependent on preferential diffusion of H_2; a flame with unity Lewis number could also propagate at such ϕ, and we call those "kinetic-controlled" flames. Preferential diffusion of H_2 is found to stabilize the "diffusion-controlled" lean hydrogen flames (when $\phi \leq 0.2$), while it destabilizes the "kinetic-controlled" lean hydrogen flames (when $\phi \geq 0.25$). Fig. 3 shows a sketch of the stabilization mechanism

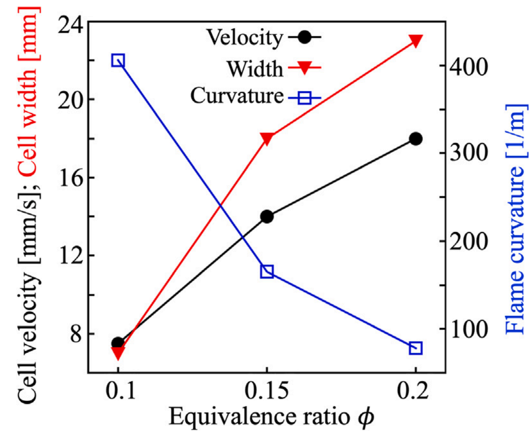

Fig. 4. Stable flame cell velocity, cell width, and critical flame curvature for the flames with different values of ϕ.

of the diffusion-controlled hydrogen flames. For a specific positive curvature κ_s, the differential diffusion effect leads to a local focusing of H_2 and to a higher local ϕ, so that the flame is able to burn locally. As the flame propagates outwards, the flame curvature κ will decrease below κ_s, resulting in a decreased differential diffusion focusing effect and attenuated local reactivity. Therefore, the flame will start to quench back with increased κ, as shown in the left of Fig. 3. Conversely, for $\kappa > \kappa_s$, the flame will accelerate until reaching again $\kappa = \kappa_s$. Therefore, each stable flame in Fig. 2 sustains a specific shape and curvature, with a single stable value of κ_s. This explains the uniqueness of the flame shape for ultra-lean diffusion-controlled 2D premixed H_2/air flames.

Fig. 4 shows the corresponding flame cell velocity, cell width and critical flame curvature κ_s for the stable flames at $\phi = 0.1, 0.15$ and 0.2. The flame cell velocity was determined by tracking the most reactive point (P) on the flame front, with the velocity

$$U = \frac{\left| \boldsymbol{X}_{\boldsymbol{P}}(t_2) - \boldsymbol{X}_{\boldsymbol{P}}(t_1) + \int_{t_1}^{t_2} \boldsymbol{u}_{\boldsymbol{inlet}}(t)dt \right|}{t_2 - t_1} \quad (1)$$

where $\boldsymbol{X}_{\boldsymbol{P}}$ is the physical coordinate of the most reactive point P (flame tip in Fig. 2) and $\boldsymbol{u}_{\boldsymbol{inlet}}$ is the adaptive inlet velocity. In our tests, the choice of the time period (t_1 and t_2) did not affect noticeably the calculation of the stable cell velocity. The critical flame curvature was tracked at the same point P with

$$\kappa_s = \frac{\int_{t_1}^{t_2} \kappa_P dt}{t_2 - t_1} \quad (2)$$

where $\kappa_P = \boldsymbol{\nabla} \cdot \boldsymbol{n}_{\boldsymbol{P}}$ and $\boldsymbol{n}_{\boldsymbol{P}}$ is the flame normal unit vector at point P. The flame cell width was roughly estimated by measuring the distance between two points on the flame front with $Q = Q_{max}/4$, where Q denotes the HRR and Q_{max} is the maximum HRR at point P. This HRR threshold was determined by a visual analysis of the flames in Fig. 2. It is seen that when ϕ decreases, both the cell velocity and cell width decrease, while the critical flame curvature increases. This is as expected because a leaner flame with smaller ϕ is less reactive, propagating slower, requiring a larger flame curvature and a smaller cell width for a more intense differential diffusion focusing effect. Fig. 4 provides a quantitative characterization of the ultra-lean flame cell features, which will constitute a starting reference for future studies.

It was reported in [4] that the stable cell width at $\phi = 0.2$ depends on the domain width. Fig. 5 shows the distribution of the local equivalence ratio ϕ_l for the stable flames. As can be seen, at $\phi = 0.2$, a strong defocusing effect of H_2 occurs beside the stable flame front, making the mixtures there extremely lean and limiting the flame propagation in the lateral direction. If the domain width would be even smaller (e.g. 20–45 mm, as in [4]), it is expected that the defocusing effect

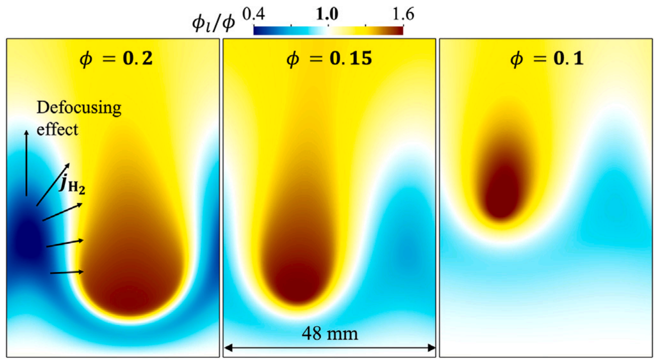

Fig. 5. Distribution of the local equivalence ratio ϕ_l (normalized by the global equivalence ratio ϕ) for the flames with ϕ = 0.2, 0.15 and 0.1 (from left to right).

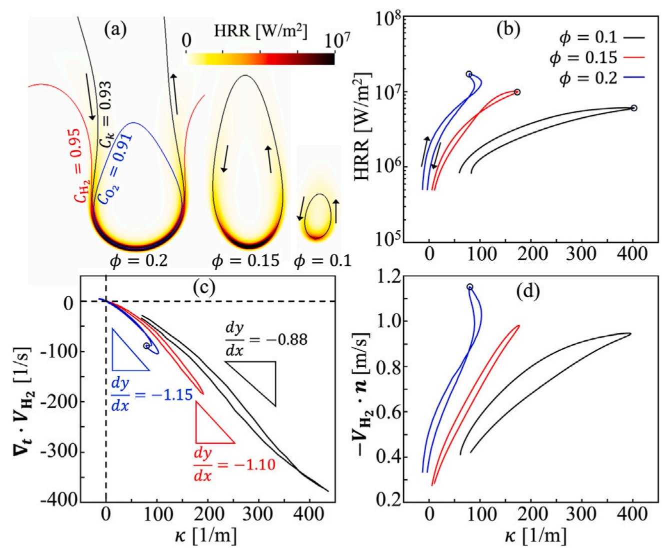

Fig. 6. (a) Choice of a proper progress variable and distributions of (b) HRR, (c) $\nabla_t \cdot V_{H_2}$, and (d) $-V_{H_2} \cdot n$ versus flame curvature κ along the flame front (represented by $C_k = 0.93$).

beside the flame cell would become more intense so that the flame cell width should decrease. This explains the results observed in [4]. At $\phi = 0.15$ or 0.1, the defocusing effect of H_2 beside the stable flame cell is less intense, since the cell width is much smaller than that at $\phi = 0.2$. This means that the observed cell widths at $\phi = 0.15$ and 0.1 are less dependent on the domain width. This confirms that the width of the numerical domain used in the present study is sufficient for all cases considered.

Since flame curvature is the key quantity for diffusion-controlled stable flames, it is important to study the dynamics of flame curvature. For this purpose, a progress variable $C_k = (Y_{k,u} - Y_k)/(Y_{k,u} - Y_{k,min})$ with $Y_k = 20 \times Y_{H_2} + Y_{O_2}$ is chosen, which could best match the peak HRR region (corresponding to $C_k = 0.93$), as seen in Fig. 6. A large weighting factor was chosen for Y_{H_2} because the reactivities of these ultra-lean flames are highly dependent on H_2 mass diffusivity. Other choices of C_k would deviate from the most relevant part of the cell flame front. This progress variable was also found to be suitable for all other ultra-lean flames with gravity, demonstrating its robustness in the ultra-lean regime. Therefore, in the following, the flame front is defined as $C_k = 0.93$. Fig. 6 shows the change of HRR, flame tangential diffusion strain rate, and flame normal diffusion velocity versus flame curvature along the flame front. The flame tangential diffusion strain rate is calculated as

$$\nabla_t \cdot V_{H_2} = \nabla \cdot V_{H_2} - n \cdot (\nabla V_{H_2}) \cdot n \tag{3}$$

where $n = -\nabla C_k/|\nabla C_k|$ is the flame normal vector pointing to the unburned gas side and V_{H_2} is the molecular diffusion velocity of H_2 calculated as [23]

$$V_{H_2} = -\frac{D^m_{H_2}}{X_{H_2}}\nabla X_{H_2} - \frac{D^s_{H_2}}{T}\nabla T + \sum_{i=1}^{N_s} Y_i \frac{D^m_i}{X_i}\nabla X_i + \frac{\nabla T}{T}\sum_{i=1}^{N_s} D^s_i Y_i. \tag{4}$$

Here D^m_i and D^s_i are the diffusion coefficients for concentration gradient diffusion and Soret diffusion respectively. The flame curvature is $\kappa = \nabla \cdot n$ (with positive value corresponding to convex flame front). In this study, $\nabla_t \cdot V_{H_2}$ represents the divergence of the molecular diffusion in flame tangential direction and can therefore be used to quantify the differential diffusion focusing effect of H_2 at positive curvatures. The flame normal diffusion velocity $V_{H_2} \cdot n$ is used to quantify the flame normal differential diffusion effect. As is seen in Fig. 6(b), HRR is monotonically dependent on κ in flames with $\phi = 0.1$ and 0.15, while it becomes non-monotonic in the flame with $\phi = 0.2$: the peak HRR location is not coincident any more with the peak curvature location at $\phi = 0.2$. HRR is directly related to chemical reaction rates, which are limited by the available amount of fuel H_2 in these ultra-lean flames. Therefore, HRR is largely determined by H_2 mass diffusion. It is necessary to examine how flame curvature affects the H_2 differential diffusion in order to interpret the observations in Fig. 6(b). In Fig. 6(c), it is observed that $\nabla_t \cdot V_{H_2}$ is almost linearly dependent on κ in all cases. As ϕ decreases, the dependency slope decreases slightly. This means that the differential diffusion focusing effect becomes less sensitive to curvature as ϕ decreases. Overall, a larger positive κ indicates more intense differential diffusion focusing effect (with a negative value of $\nabla_t \cdot V_{H_2}$ indicating a convergence of the diffusion flux). Interestingly, $\nabla_t \cdot V_{H_2}/\kappa \approx$ -1 m/s in all these ultra-lean H_2 flames, providing a quantitative measure of the differential diffusion focusing effect as a function of flame curvature. To investigate the underlying physical meaning of this scaling, we consider first a simple laminar spherical flame. In this case, the tangential strain rate due to flame propagation is

$$\nabla_t \cdot u = \kappa S_n \tag{5}$$

where S_n is the flame speed. H_2 diffusion velocity is very similar to the flame speed, and both are normal to the flame front. Therefore, we can replace the flame speed with H_2 diffusion velocity in Eq. (5). Then

$$\nabla_t \cdot V_{H_2} = \kappa V_{H_2,n} \tag{6}$$

where $V_{H_2,n} = V_{H_2} \cdot n$ is the H_2 diffusion velocity in flame normal direction. Therefore, the scaling $\nabla_t \cdot V_{H_2}/\kappa$ is closely related to the flame normal H_2 diffusion velocity. This relationship is evident when comparing Fig. 6(c) and (d). The scaling values in Fig. 6(c) approximate well $V_{H_2} \cdot n$ at the critical curvatures in Fig. 6(d), with a value close to -1 m/s. Note that this scaling law with $V_{H_2,n}$ is not expected to depend on any specific flame or working condition. It should be a general approximate scaling for hydrogen flames to study the link between curvature and differential diffusion focusing. For a general application (outside of the ultra-lean regime), we could approximate $V_{H_2,n}$ using a 1D laminar planar flame solution. This scaling would thus become useful for modeling turbulent flames. The validity of this modeling approach will be checked in our next studies.

On the other hand, in Fig. 6(d), $V_{H_2} \cdot n$ also seems to be roughly linearly dependent on κ in flames with $\phi = 0.1$ and 0.15. This is because the most strongly curved flame element (with large κ) propagates farther into the fresh gas, with a larger species gradient, therefore a larger flame normal diffusion velocity. In the flame with $\phi = 0.2$, the flame elements with peak κ appear at the left/right bottom corners, while

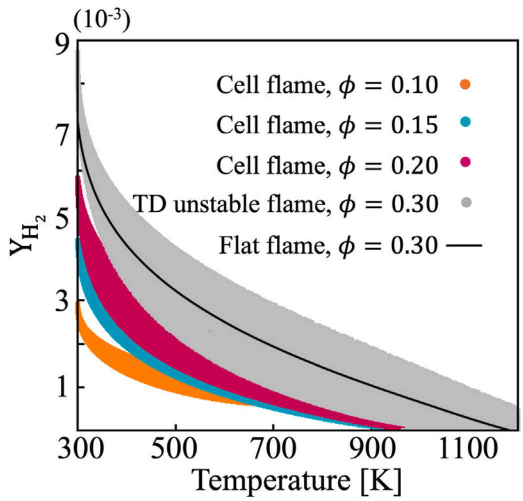

Fig. 7. Scatter plot of the thermochemical space (represented by temperature and Y_{H_2}) for the stable cell flames at $\phi = 0.1, 0.15$, 0.2, and thermodiffusive (TD) unstable flame at $\phi = 0.3$. The flat flame at $\phi = 0.3$ is also plotted for comparison.

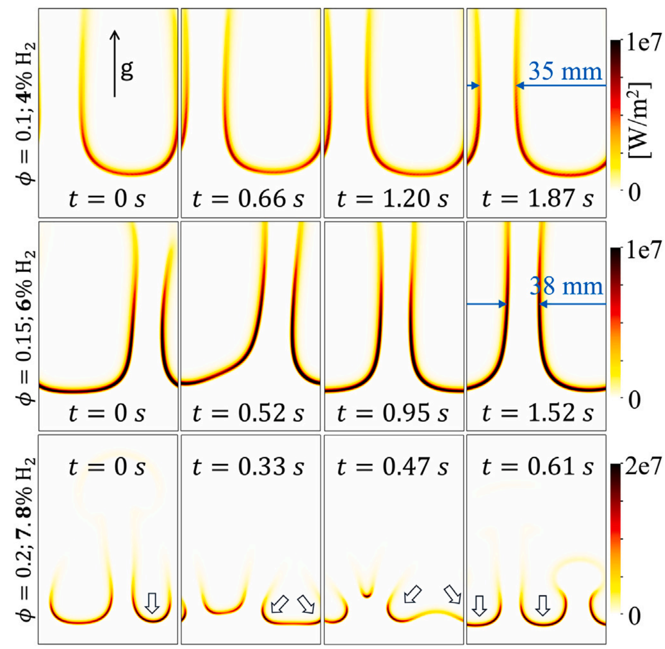

Fig. 8. Temporal evolution of the flame propagation for the lean hydrogen flames with $\phi = 0.1, 0.15$ and 0.2 from top to bottom. Flame propagates from top to bottom, with gravity ($g = 9.8$ m/s^2) in the opposite direction.

the flame near the center propagates even farther into the fresh gases. That is why the peak $\boldsymbol{V}_{H_2} \cdot \boldsymbol{n}$ does not coincide exactly with the peak curvature at $\phi = 0.2$. In general, both $\nabla_t \cdot \boldsymbol{V}_{H_2}$ and $\boldsymbol{V}_{H_2} \cdot \boldsymbol{n}$ are closely related to the HRR on the flame front of these diffusion-controlled stable flames. In the flame at $\phi = 0.2$, the enhanced flame normal diffusion at the far end of the flame contributes more to HRR than the enhanced differential diffusion focusing effect at the side corners, resulting in a non-monotonic trend of HRR with κ as observed in Fig. 6(b). As ϕ decreases, the differential diffusion focusing effect becomes more and more significant, with larger flame curvature, contributing to largely decreased $\nabla_t \cdot \boldsymbol{V}_{H_2}$ (increase of the absolute value). That is why a more monotonic trend of HRR with κ is observed for the flames at $\phi = 0.1$ and 0.15.

After analyzing the flame shape and flame curvature of the stable ultra-lean cell flames, it is valuable to examine the thermochemical space of these flames. Fig. 7 shows the scatter plot of the thermochemical space for the stable cell flames at $\phi = 0.1$, 0.15 and 0.2. The flat flame at $\phi = 0.3$ is also plotted. It is observed that the thermochemical spaces of these ultra-lean cell flames for $\phi \le 0.2$ lay outside the region delimited by the lean flat flames. This is well expected since the flat flames cannot reach a leaner condition with $\phi \le 0.2$. However, for the thermodiffusive unstable lean hydrogen flames, the flame elements can reach a leaner condition due to curvature, as shown in Fig. 7. These ultra-lean stable cell flames provide a modeling basis for the unstable flames, since they cover the lean burning limit for such flames. Therefore, these cell flames largely extend the classical flamelet composition space and contain important additional information, highly relevant for modeling lean H_2/air flames.

3.2. Flame propagation with gravity

It was reported in [11] that gravity largely affects the ultra-lean flame shape. Therefore, this section examines the effect of gravity on the ultra-lean H_2 flames. Fig. 8 shows the time evolution of flame propagation with gravity in the opposite direction (from bottom to top). At $\phi = 0.25$ and 0.3, the flames become unstable, so they are not shown. As seen, the flame cell widths are largely increased at $\phi = 0.1$ and 0.15, due to the opposed gravity. At $\phi = 0.2$, a flame branching process is observed, supported by gravity. The single-flame cell splits into two separate cells. This phenomena is quite similar to the splitting cells observed in experiments for narrow gap flames [11].

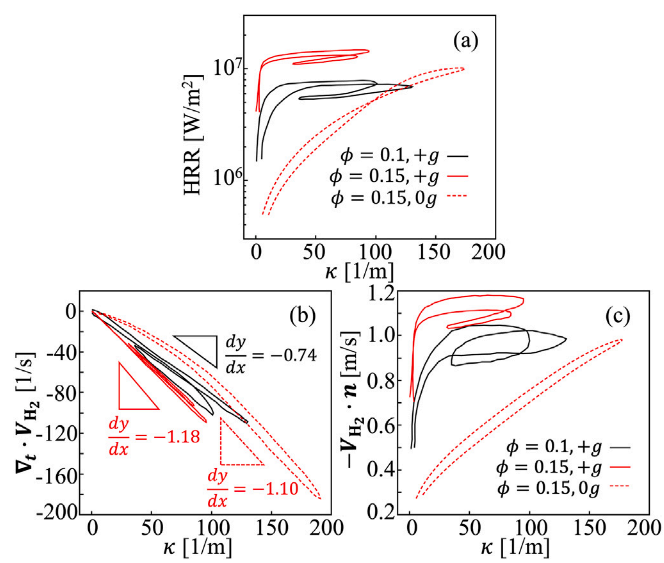

Fig. 9. Distributions of (a) HRR, (b) $\nabla_t \cdot \boldsymbol{V}_{H_2}$, and (c) $-\boldsymbol{V}_{H_2} \cdot \boldsymbol{n}$ versus curvature κ along the flame front for the flames at $\phi = 0.1$ and 0.15 with gravity in the opposite direction ($+g$). The results for the flame at $\phi = 0.15$ without gravity ($0g$) are also plotted.

To understand the flame shape observed in Fig. 8, the flame curvature is analyzed. Fig. 9 depicts the distributions of HRR, $\nabla_t \cdot \boldsymbol{V}_{H_2}$, and $\boldsymbol{V}_{H_2} \cdot \boldsymbol{n}$ versus flame curvature along the flame front. As is seen, the HRR becomes less dependent on κ. Similar to the flames with zero gravity, a nearly linear relationship between $\nabla_t \cdot \boldsymbol{V}_{H_2}$ and κ is observed in Fig. 9(b). The slopes are also quite similar for the cases with and without gravity. This means that gravity has only limited effect on the differential diffusion focusing effect. However, the effect of gravity on $\boldsymbol{V}_{H_2} \cdot \boldsymbol{n}$ is obvious, as seen in Fig. 9(c), the quantity $\boldsymbol{V}_{H_2} \cdot \boldsymbol{n}$ being now less dependent on flame curvature. To explain this observation, a direct visualization of the distribution of $|\boldsymbol{V}_{H_2} \cdot \boldsymbol{n}|$ in the computational

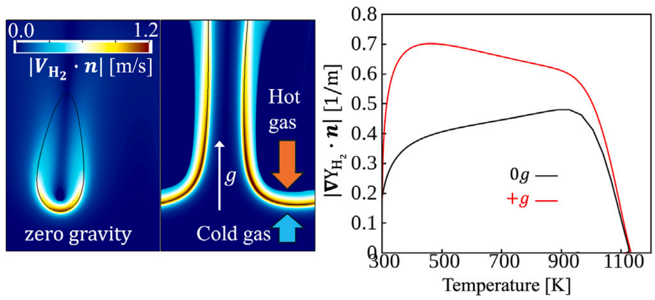

Fig. 10. (Left) The spatial distributions of $|V_{H_2} \cdot n|$ for the flames at $\phi = 0.15$ with and without gravity and (Right) gradient of Y_{H_2} in flame normal direction along the flame front for the flame tips with and without gravity.

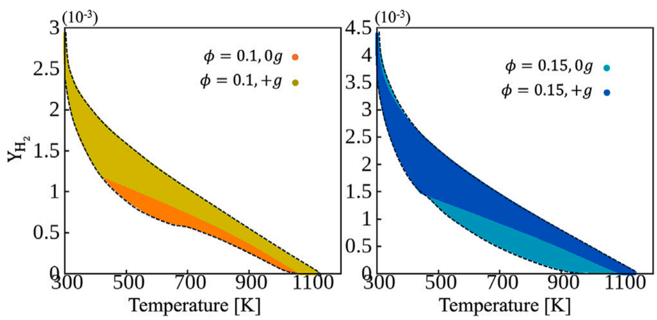

Fig. 11. Scatter plot of the thermochemical space for the stable cell flames at $\phi = 0.1$ (left) and $\phi = 0.15$ (right) with (yellow, dark blue) and without gravity (orange, light blue). The dashed lines indicate the boundary of the thermochemical space for flames without gravity.

domain is shown in Fig. 10. The flame normal differential diffusion is shown to be intensified after imposing gravity. This is because the gravity pushes hot gases downward and fresh gases upward, resulting in a steeper species gradient and therefore a larger diffusion flux. Fig. 10 shows the species (H_2) gradient along the flame front for the flame tips with and without gravity. The enhanced species gradient due to gravity is obvious, supporting the previous explanation. The enhanced flame normal differential diffusion results in an enhanced flame reactivity. Finally, the flame propagates outwards, with a larger cell width and smaller κ, and sustains its shape due to the enhanced reactivity. The dominant role of flame normal differential diffusion can also be seen when comparing the flames at $\phi = 0.1$ and 0.15 in Fig. 9. $|V_{H_2} \cdot n|$ is obviously smaller at smaller ϕ, while $\nabla_t \cdot V_{H_2}$ stays comparable in both cases. Therefore, with opposite gravity, the effect of flame curvature becomes less dominant.

At $\phi = 0.2$, the flame elements at the two bottom corners are much more reactive and burn faster, splitting the single flame cell into two small cells. The two small cells have higher κ, with intense focusing effect and much higher HRR, especially at the two bottom corners of each cell. These two corners then propagate much faster than the other flame elements and soon form again two new cells. In this scenario, the curvature-induced reactivity enhancement is dominating the flame propagation, which is very similar to the behavior of thermodiffusive unstable flames. This explains the splitting cell phenomena, as also observed in [11].

The thermochemical spaces of the stable cell flames with opposite gravity are examined and compared to the flames without gravity in Fig. 11. It is obvious that the thermochemical states of the flames with gravity are mostly included by the states of the flames without gravity. Gravity compresses the thermochemical states in the flame zone.

Finally, ultra-lean flame propagation with gravity in the same direction (i.e., from top to bottom) is examined. Fig. 12 shows corresponding

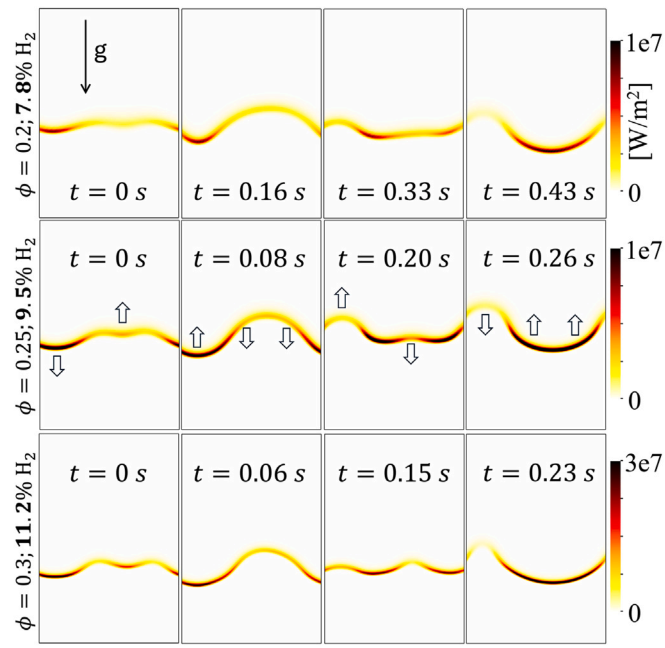

Fig. 12. Flame propagation for lean hydrogen flames with equivalence ratio $\phi = 0.2, 0.25$ and 0.3 from top to bottom. Flame propagates from top to bottom, with gravity ($g = 9.8$ m/s^2) in the same direction.

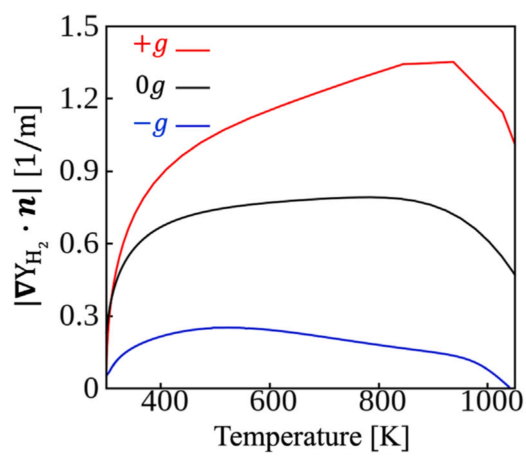

Fig. 13. Gradient of Y_{H_2} in flame normal direction along the flame front for the flame tips at $\phi = 0.2$ with and without gravity.

flame propagation. In this case, the flames at $\phi = 0.1$ and 0.15 cannot sustain and quench. The flames at $\phi = 0.2$, 0.25 and 0.3 show several unstable cells along the reaction front, and this feature persists in time. This is because gravity tends to decrease the species gradient and reduce the molecular diffusion effect. Fig. 13 shows the H_2 species gradient across the flame front with and without gravity. The effect of gravity on species gradient is obvious. The slow flame time scale of these ultra-lean flames (0.05~0.2 s) becomes comparable to the time scale of the buoyancy-driven flow (~0.1 s). Therefore, the buoyant flow induced by negative gravity (blue line in Fig. 13) pushes the hot burned gases and cold fresh gases away from the flame front, reducing the species gradient. For the diffusion-controlled flames (at $\phi = 0.1$ and 0.15), the attenuated differential diffusion effect directly results in flame quenching. Richer flames (at $\phi \geq 0.2$) can sustain, but become unstable. Similar unstable flame patterns are observed for the flames at different ϕ. First, the far-end positive κ flame element propagates and expands, while the other flame elements quench back. As κ of this far-end flame element decreases, the differential diffusion focusing effect is reduced and this flame element will quench back as well (see arrows in Fig. 12 for $\phi = 0.25$). Then, a two-headed cell from the other flame elements propagates to the far end. This two-headed cell then forms a larger one-headed cell and this larger cell will quench back again due to the small κ. These 2D results are different from the narrow-gap flame results where two-headed steady cells are observed [11]. This means that heat loss (to the wall, instead of convection) is critical for the two-headed cell stabilization mechanism. Future studies should try to reveal this specific mechanism.

3.3. Generality of the findings in more realistic configurations

All previous findings have been obtained using the 2D configuration. However, real configurations are always 3D, usually combined with a turbulent flow and also wall confinement. It is therefore of practical significance to discuss the generality of the above findings in more realistic configurations.

Firstly, the ultra-lean diffusion-controlled flame stabilization mechanism should also apply for a 3D flame. For both 2D and 3D flames, the flame stabilization will be achieved when the lateral heat loss balances the chemical heat release due to enhanced hydrogen mass diffusion at positive curvature. Compared to the 2D flame, the 3D flame is expected to have more heat loss in lateral directions (due to additional heat loss in z direction). Therefore, the critical curvature should be larger (resulting in enhanced local reactivity to compensate the additional heat loss in z direction), with a smaller cell width for the 3D flame compared to the 2D flame at the same equivalence ratio. This may also change the limits of the flame propagation modes shown in Fig. 1. For instance, the 3D flame may already extinguish at $\phi = 0.1$ without gravity. Possible quantitative effects need to be verified in future studies. Due to the very long physical time duration needed for the ultra-lean flames, corresponding 3D flame simulations will be very expensive and challenging.

The effect of wall confinement has already been studied recently in [22]. It was observed that there is a negligible role of wall confinement on the ultra-lean flame propagation characteristics. Therefore, we can infer that the above findings should also work for configurations with wall confinement.

The effect of turbulence is expected to be very complicated. Turbulence will potentially change the flame shape, perturbing the establishment of a stable flame curvature, possibly enhancing flame quenching. Dedicated investigations are necessary to clarify this point.

4. Conclusions

The present study investigates ultra-lean diffusion-controlled premixed hydrogen/air flames in a 2D configuration with and without gravity. Different equivalence ratios from 0.1 to 0.3 are considered. The main findings are as follows

- Without gravity, stable flame cells were observed when $0.1 \leq \phi \leq 0.2$. The stable cell width becomes smaller for lower ϕ.
- The flame curvature linearly affects the differential diffusion focusing. At a smaller ϕ, a larger flame curvature is needed to retain a certain flame reactivity.
- As ϕ decreases, the differential diffusion focusing effect (quantified by tangential diffusion) becomes more important than flame normal differential diffusion.
- With opposite gravity, the flame normal differential diffusion is intensified and becomes the dominant mechanism for flame stabilization. The flame at $\phi = 0.2$ exhibits a splitting cell feature.
- When gravity is imposed in the same direction as flame propagation, the ultra-lean flames at $\phi \leq 0.15$ cannot sustain, and the flames at $\phi = 0.2$, 0.25 and 0.3 become unstable.
- Stable two-headed flame cells were not observed in these 2D flame simulations, proving the importance of wall heat loss for this specific flame mode.

These findings are important for a better understanding of the interesting flame cell propagation modes under ultra-lean conditions and support the reduced-order model development for ultra-lean premixed flames. Future studies would examine the 3D ultra-lean diffusion-controlled premixed hydrogen flames and the effect of turbulence on such flames.

CRediT authorship contribution statement

Cheng Chi: Performed research, Analyzed data, Wrote paper. **Zheng Chen:** Reviewed paper. **Dominique Thévenin:** Reviewed paper, Funding.

Declaration of competing interest

The authors declare that they have no known competing financial interests or personal relationships that could have appeared to influence the work reported in this paper.

Acknowledgments

C. Chi would like to thank the DFG, Germany for its support within Project TH881/38-1 (DADOREN), and acknowledges the computational resources provided by the Jülich Supercomputing centre (JSC) under Grant "dadoren".

References

[1] H. Pitsch, The transition to sustainable combustion: Hydrogen- and carbon-based future fuels and methods for dealing with their challenges, Proc. Combust. Inst. 40 (1) (2024) 105638.
[2] A.J. Aspden, M.S. Day, J.B. Bell, Turbulence–flame interactions in lean premixed hydrogen: transition to the distributed burning regime, 2011/05/31, J. Fluid Mech. 680 (2011) 287–320.
[3] L. Berger, K. Kleinheinz, A. Attili, H. Pitsch, Characteristic patterns of thermodiffusively unstable premixed lean hydrogen flames, Proc. Combust. Inst. 37 (2) (2019) 1879–1886.
[4] J.F. Grcar, A new type of steady and stable, laminar, premixed flame in ultra-lean, hydrogen–air combustion, Proc. Combust. Inst. 32 (1) (2009) 1011–1018.
[5] P.D. Ronney, Near-limit flame structures at low lewis number, Combust. Flame 82 (1) (1990) 1–14.
[6] J. Buckmaster, P. Ronney, Flame-ball drift in the presence of a total diffusive heat flux, Symp. (International) Combust. 27 (2) (1998) 2603–2610.
[7] H. Du, W.S. Chai, H. Wei, L. Zhou, Status and challenges for realizing low emission with hydrogen ultra-lean combustion, Int. J. Hydrog. Energy 57 (2024) 1419–1436.
[8] Y.L. Shoshin, J.A. van Oijen, A.V. Sepman, L.P.H. de Goey, Experimental and computational study of the transition to the flame ball regime at normal gravity, Proc. Combust. Inst. 33 (1) (2011) 1211–1218.
[9] R. Fursenko, S. Minaev, H. Nakamura, T. Tezuka, S. Hasegawa, K. Takase, X. Li, M. Katsuta, M. Kikuchi, K. Maruta, Cellular and sporadic flame regimes of low-lewis-number stretched premixed flames, Proc. Combust. Inst. 34 (1) (2013) 981–988.
[10] F.E. Hernández-Pérez, B. Oostenrijk, Y. Shoshin, J.A. van Oijen, L.P.H. de Goey, Formation, prediction and analysis of stationary and stable ball-like flames at ultra-lean and normal-gravity conditions, Combust. Flame 162 (4) (2015) 932–943.
[11] F. Veiga-López, M. Kuznetsov, D. Martínez-Ruiz, E. Fernández-Tarrazo, J. Grune, M. Sánchez-Sanz, Unexpected propagation of ultra-lean hydrogen flames in narrow gaps, Phys. Rev. Lett. 124 (17) (2020) 174501.
[12] J. Yáñez Escanciano, M. Kuznetsov, F. Veiga-López, Characterization of unconventional hydrogen flame propagation in narrow gaps, Phys. Rev. E 103 (3) (2021) 033101.
[13] P.V. Moskalev, V.P. Denisenko, I.A. Kirillov, Classification and dynamics of ultralean hydrogen–air flames in horizontal cylindrical hele–shaw cells, J. Exp. Theor. Phys. 137 (1) (2023) 104–113.
[14] D. Fernández-Galisteo, V.N. Kurdyumov, P.D. Ronney, Analysis of premixed flame propagation between two closely-spaced parallel plates, Combust. Flame 190 (2018) 133–145.

[15] D. Martínez-Ruiz, F. Veiga-López, D. Fernández-Galisteo, V.N. Kurdyumov, M. Sánchez-Sanz, The role of conductive heat losses on the formation of isolated flame cells in Hele-Shaw chambers, Combust. Flame 209 (2019) 187–199.

[16] A. Domínguez-González, D. Martínez-Ruiz, M. Sánchez-Sanz, Stable circular and double-cell lean hydrogen-air premixed flames in quasi two-dimensional channels, Proc. Combust. Inst. 39 (2) (2023) 1731–1741.

[17] A. Domínguez-González, M.P. Encinar, D. Martínez-Ruiz, Pathway dynamics to double-cell premixed flames in lean hydrogen–air mixtures, Proc. Combust. Inst. 40 (1) (2024) 105496.

[18] L. Yang, Y. Wang, T. Zhang, X. Gou, W. Kong, Z. Chen, Propagation of ultra-lean hydrogen/air flames in a Hele-Shaw cell, Combust. Flame 281 (2025) 114444.

[19] J. Yanez, L. Kagan, G. Sivashinsky, M. Kuznetsov, Modeling of 2D self-drifting flame-balls in hele-shaw cells, Combust. Flame 258 (2023) 113059.

[20] A. Abdelsamie, G. Fru, T. Oster, F. Dietzsch, G. Janiga, D. Thévenin, Towards direct numerical simulations of low-Mach number turbulent reacting and two-phase flows using immersed boundaries, Comput. Fluids 131 (2016) 123–141.

[21] P. Boivin, C. Jiménez, A.L. Sánchez, F.A. Williams, An explicit reduced mechanism for H2–air combustion, Proc. Combust. Inst. 33 (1) (2011) 517–523.

[22] E. Fernández-Tarrazo, R. Gómez-Miguel, M. Sánchez-Sanz, Exploring the survival of premixed hydrogen flames below the lean flammability limit, Combust. Flame 279 (2025) 114315.

[23] C. Chi, W. Han, D. Thévenin, Effects of molecular diffusion modeling on turbulent premixed NH3/H2/air flames, Proc. Combust. Inst. 39 (2) (2023) 2259–2268.